Beam test of the silicon timing for use in calorimetry.

A. Apresyan[1], G. Bolla[2], H. Kim[3], S. Los[2], C. Pena[1], F. Presutti[1], E. Ramberg[2], A. Ronzhin[2], M. Spiropulu[1], and S. Xie[1]

[1] *California Institute of Technology, Pasadena, CA, USA*
[2] *Fermi National Accelerator Laboratory, Batavia, IL, USA*
[3] *University of Chicago, Chicago, IL, USA*

Abstract

The high luminosity upgrade of the Large Hadron Collider (HL-LHC) at CERN is expected to provide instantaneous luminosities of 5×10^{34} cm^{-2} s^{-1}. The high luminosities expected at the HL-LHC will be accompanied by a factor of 5 to 10 more pileup compared with LHC conditions in 2015, causing general confusion for particle identification and event reconstruction. Precision timing allows to extend calorimetric measurements into such a high density environment. Calorimeters employing silicon as the active component have recently become a popular choice for the HL-LHC and future collider experiments which face very high radiation environments. In this article, we present studies of calorimetric and precision timing measurements using a prototype composed of tungsten absorber and silicon pad sensors as the active medium. We show that for the bulk of electromagnetic showers induced by electrons in the range of 20 GeV to 30 GeV, we can achieve time resolutions better than 25 ps.

1 Introduction

Future hadron colliders, including the high luminosity upgrade of the Large Hadron Collider (HL-LHC) at CERN, will require improvements to the instantaneous luminosity by an order of magnitude or more compared to what has been achieved at the LHC so far. With the increased instantaneous luminosity, it is expected that the pileup, multiple collisions occurring simultaneous in time, will increase correspondingly by a factor of 5 to 10. This increased pileup will result in significantly increased particle densities, causing overall confusion for particle identification and event reconstruction.

One way to mitigate the pileup confusion effects, complementary to precision tracking methods, is to perform a time of arrival measurement associated with a particular layer of the calorimeter, allowing for a time assignment for both charged particles and photons. Such a measurement with a precision of about 20-30 ps, when unambiguously associated to the corresponding energy measurement, will reduce the effective amount of pileup by a factor of 10 given that the spread in collision time of the pileup interactions is approximately 200 ps. The association of the time measurement with the energy measurement is crucial, and leads to a prototype design that calls for the time and energy measurements to be performed in the same active detector element.

We have performed past studies of alternative options to improve timing for calorimetry [**?** **?** **?** **?**]. In this article, we describe the continuation of this program of study using a calorimeter prototype employing a silicon pad sensor as the active medium. Silicon-based calorimeters have recently become a popular choice for future hadron colliders due to its radiation hardness properties. An important example is the calorimeter proposed for the CMS Phase 2 Upgrade [**?**]. We study

the timing properties of silicon-based calorimeters using a prototype composed of tungsten absorber and a silicon sensor produced by Hamamatsu [**?**].

The paper is organized as follows. General silicon timing properties and bench test results are described in Section 2. The test beam setup and experimental apparatus are presented in Section 3. The results of the test beam measurements are presented in Section 4, and Sections 5 and 6 are devoted to discussion and conclusion, respectively.

2 General Properties of Silicon Timing and Bench Test Studies

A few factors determine the timing response of silicon detectors. The time constant depends on the series resistance of the silicon, the load resistance, and the terminal capacitance. The carrier velocity and its collection time depend on the thickness of the silicon, the depletion voltage, and the type of carrier. The drift time of the carriers in fully depleted silicon determines the carriers collection time. In the case of small time constant, the time response of the silicon sensor is determined by the collection time, however for silicon with large capacitance the time response depends mostly on the time constant.

For our measurements, we used a silicon sensor produced by Hamamatsu [**?**]. The thickness of the silicon was measured to be 325 μm. The transverse size of the silicon is 6x6 mm^2. The negative bias voltage was applied to p-side of the silicon. The dependence of the diode capacitance on the bias voltage is presented in Figure 1. The junction capacitance depends on the area of p-layer and the thickness of the depletion layer which increases with reverse bias voltage. When charged particles pass through the silicon the electrons produced are collected on the n-side of the silicon, opposite to the p-side, and forms the output signal. The electrical schematics of the silicon diode are presented in Figure 1.

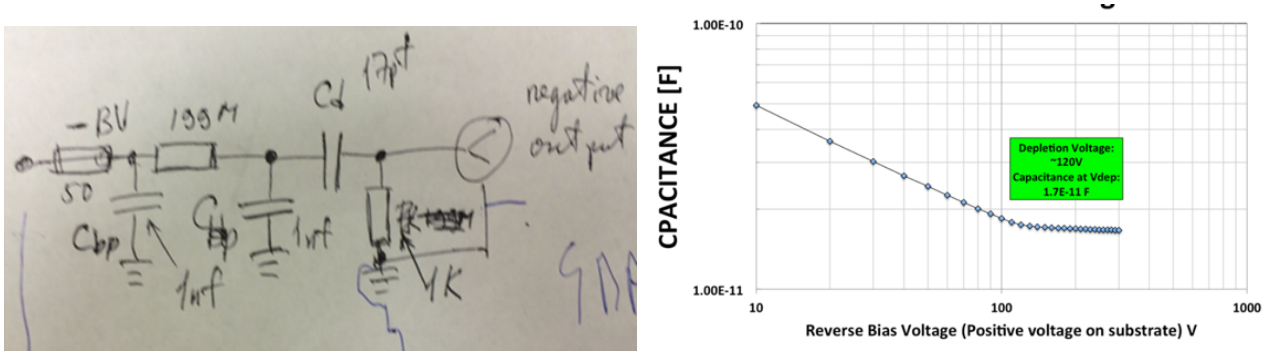

Figure 1: The electrical schematics of the silicon diode is shown on the left. The measured capacitance as a function of the applied bias voltage is shown on the right.

The silicon diode was placed inside a metal box of thickness 1.5 cm. The HV was applied to the printed circuit board by a cable terminated by an SHV connector at the other end. The silicon diode output signal is read out through an SMA connector attached to the box. The dark current was measured as a function of the bias voltage. The maximum value of the current at -500 V of the bias was less of 1 nA. The silicon box and bench test setup are presented in Figure 2.

3 Test-beam Setup and Experimental Apparatus

We performed the test-beam measurements at the Fermilab Test-beam Facility (FTBF) which provided proton beams from the Fermilab Main Injector accelerator at 120 GeV, and secondary beams composed of electrons, pions, and muons of energies ranging from 4 GeV to 32 GeV. A simple

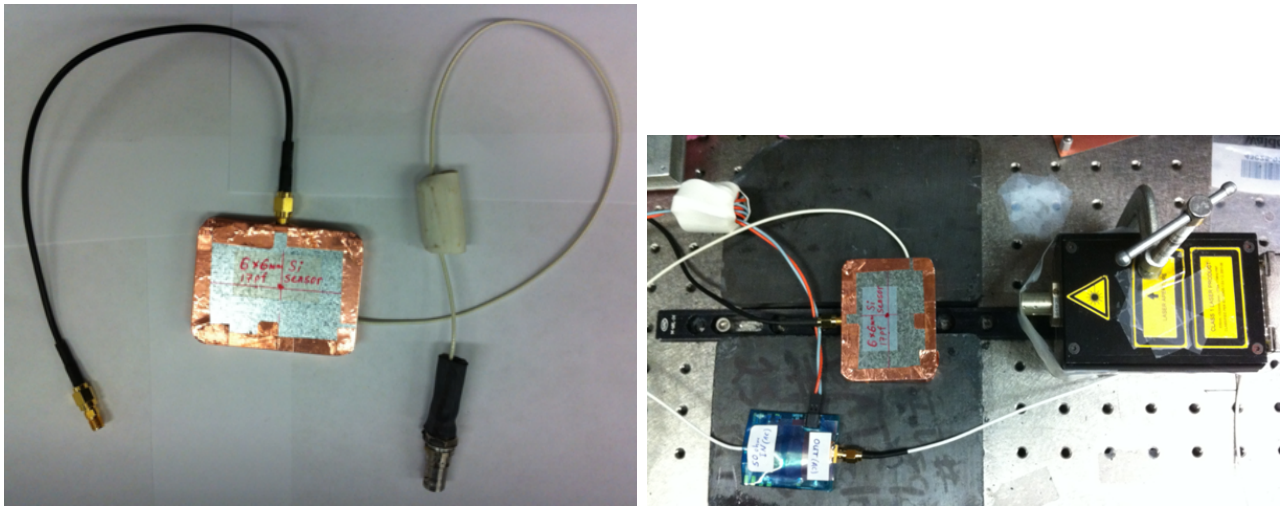

Figure 2: External view of the box with silicon diode and PC board inside (left) and bench test setup (right).

schematic diagram of the experimental setup is shown in Figure 3. A small plastic scintillator of transverse dimensions 1.8 mm×2 mm is used as a trigger counter to initiate the read out of the data acquisition (DAQ) system. It is also used to constrain the transverse beam-spot to a small geometric area. Next, we place a stack of tungsten absorbers of various thicknesses for measurements at various longitudinal locations within the electromagnetic shower. The silicon pad sensor is located within a metal box covered by copper foil, and is placed immediately downstream of the absorber plates. Finally, a Photek 240 micro-channel plate photomultiplier detector [**?** **?** **?** **?**] is placed furthest downstream, and serves to provide a very precise reference timestamp. A photograph showing the various detector components is presented in Figure 4. A differential Cherenkov counter is located further upstream of our experimental setup and can provide additional particle identification capability. More details of the experimental setup are described in our previous studies using the same experimental facility in references [**?** **?** **?** **?**].

The DAQ system is based on the CAEN V1742 digitizer board [**?**], which provides digitized waveforms sampled at 5 GS/s. The metal box containing the silicon sensor was located on a motorized X-Y moving stage allowing us to change the location of the sensor in the plane transverse to the beam at an accuracy better than 0.1 mm. A nominal bias voltage of 500 V was applied to deplete the silicon sensor. The signals from the silicon sensor were amplified by two fast and high-bandwidth pre-amplifiers connected in series. The first amplifier is an ORTEC VT120C pre-amplifier, and the second amplifier is a Hamamatsu C5595 amplifier. Using a pulse-generator, we measured the combined amplification gain of the two amplifiers in series as a function of the input signal amplitude and found some degree of non-linearity for typical signals produced by the silicon sensor under study. The measured gain ranged from 200 for signals with amplitude around 0.15 mV to 650 for signals with amplitude around 10 mV.

4 Test Beam Measurements and Results

Measurements were performed using the secondary beam at the FTBF, which provides a beam of electrons and pions. Beam energies ranging from 4 GeV/c^2 to 32 GeV/c^2 were used, for which the electron purity ranges between 70% at the lowest energy to about 10% at the highest energy. Stacks of tungsten plates with different thicknesses were placed immediately upstream of the silicon device in order to measure the response along the longitudinal direction of the electromagnetic shower. The transverse size of the tungsten plates allowed us to fully cover the transverse size of the silicon device. The signals from the silicon sensor and the Photek MCP-PMT are read out and digitized

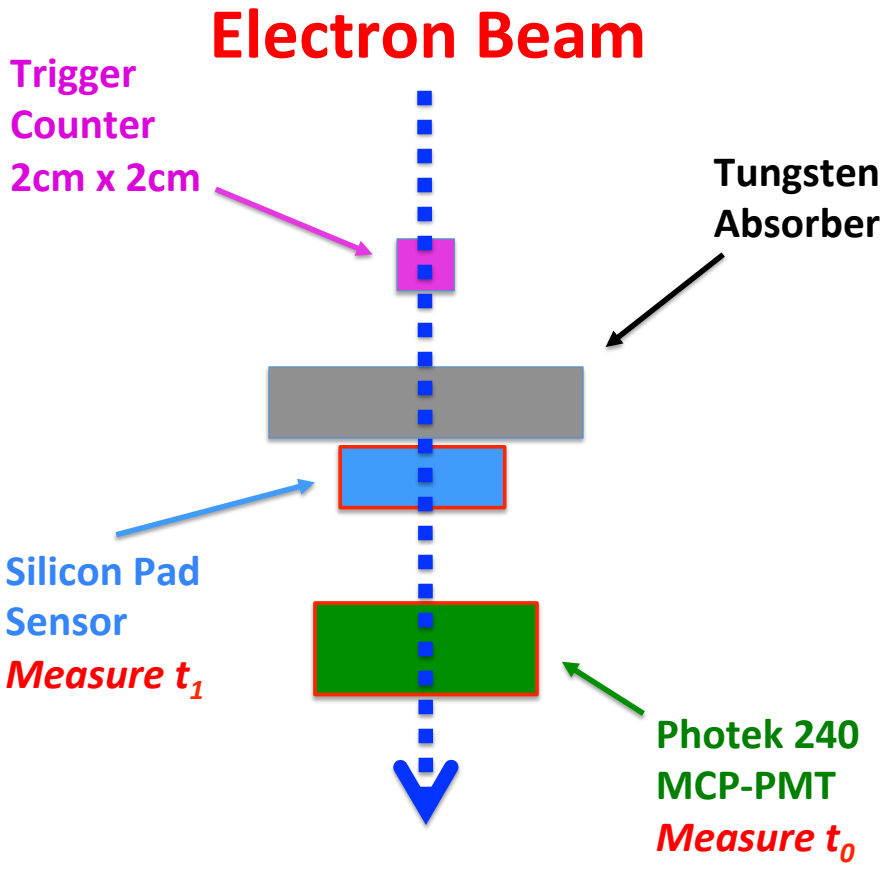

Figure 3: A schematic diagram of the test-beam setup is shown.

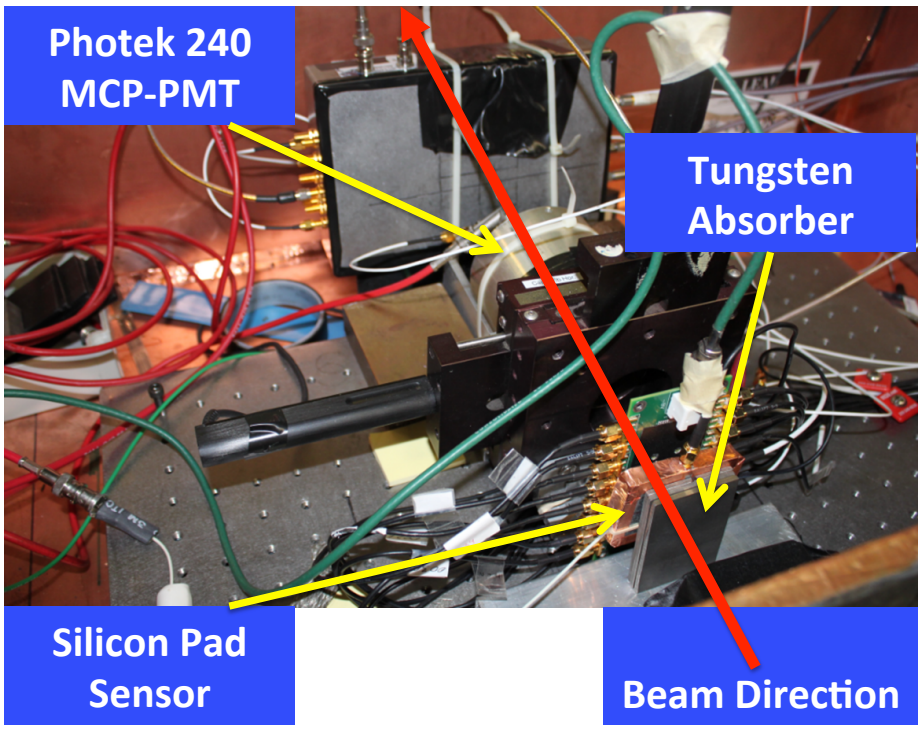

Figure 4: Test beam setup.

by the V1742 digitizer, and example signal waveforms are shown in Fig. 5. The signal pulse in the silicon sensor has a rise time of about 1.5 ns, and a full pulse width of around 7 ns.

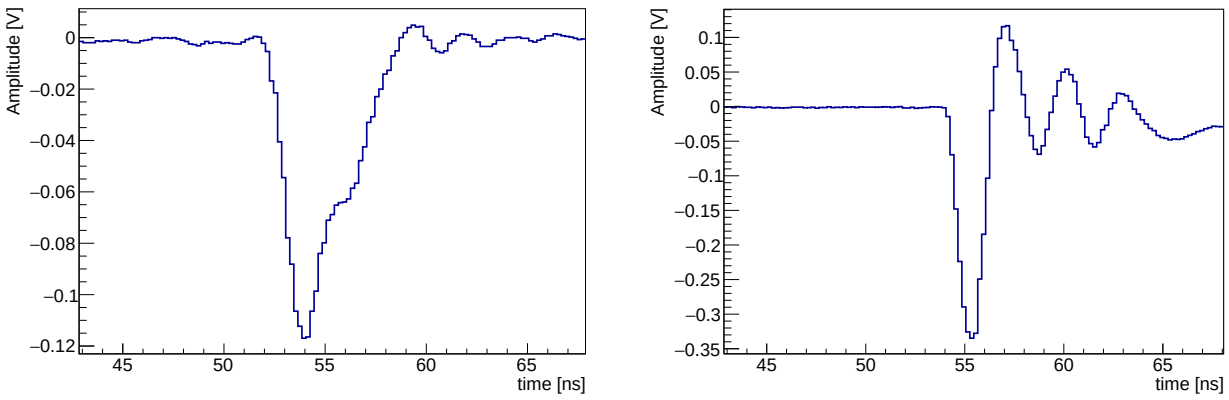

Figure 5: Examples of the signal pulse waveform for the silicon sensor (left) and the Photek MCP-PMT (right) digitized by CAEN V1742 digitizer board.

The raw waveforms are calibrated in both the voltage and time dimension using known inputs from a pulse generator [**?**]. The total collected charge for each signal pulse is computed by integrating a 10−ns window around the peak of the pulse. The time for the reference Photek MCP-PMT detector is obtained by fitting the peak region of the pulse to a Gaussian function and the mean parameter of the Gaussian is assigned as the timestamp. The time for signals from the silicon sensor is obtained by performed a linear fit to the rising edge of the pulse and the time at which the pulse reaches 30% of the maximum amplitude is assigned as its timestamp. We measured the electronic time resolution of the CAEN V1742 digitizer as ∼4 ps and neglected this impact on the timing measurements described below.

Electrons were identified using a combination of the gas Cherenkov counter provided by the FTBF and the signal size in the Photek detector located further downstream of the silicon sensor. Electromagnetic showers induced by electrons produce significantly larger signals in the Photek MCP-PMT, while pions produce a much smaller signal. After imposing the electron identification requirements the electron purity is between 80% and 90% for all beam conditions.

We begin by establishing the signal characteristics of a minimum-ionizing particle (MIP) using beams of 120 GeV protons as well as 8 GeV electrons with no absorbers upstream of the silicon pad sensor. To distinguish MIP signals from noise, we collect data events of pure noise with no beam and random triggers. The charge distribution for noise runs is presented in Fig. 6. As expected, the charge distribution for noise runs is centered at 0, and the RMS is about 2 fC.

In Figure 7, we show the response of the silicon sensor to the proton and electron beam without any absorbers upstream. We observe very similar response for these two cases, and measure an integrated charge of 4.5 fC and 5.0 fC for the proton and electron beams respectively. The measured charge takes into account the response of the amplifiers and attenuators used, which were measured in the lab using a pulse generator in the full dynamic range relevant for the current study. We expect that a MIP traversing a silicon sensor of thickness 300μm to produce roughly 32000 electron-hole pairs, corresponding to a charge of about 5.1 fC. Thus, our measured value is in close agreement with expectations. Having established the absolute scale of the measured response using MIP's, in our remaining studies we normalize all charge measurements to the charge integrated in the silicon sensor for one MIP.

We study the response of the silicon sensor to electron beams of various energies after 6 radiation lengths of tungsten absorber. The silicon sensor is expected to be sensitive to the number of secondary electrons produced within the electromagnetic shower, and therefore its response is expected to scale up with higher incident electron energy. In Figure 8, we show an example of the

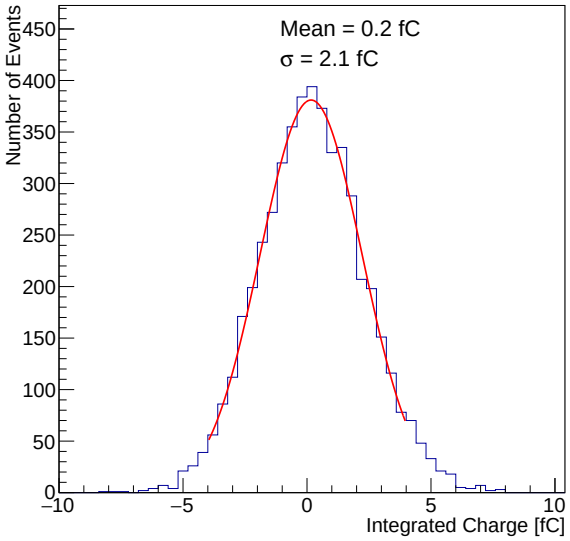

Figure 6: The distribution of charge integrated in the silicon sensor is shown for randomly triggered data recorded with no beam.

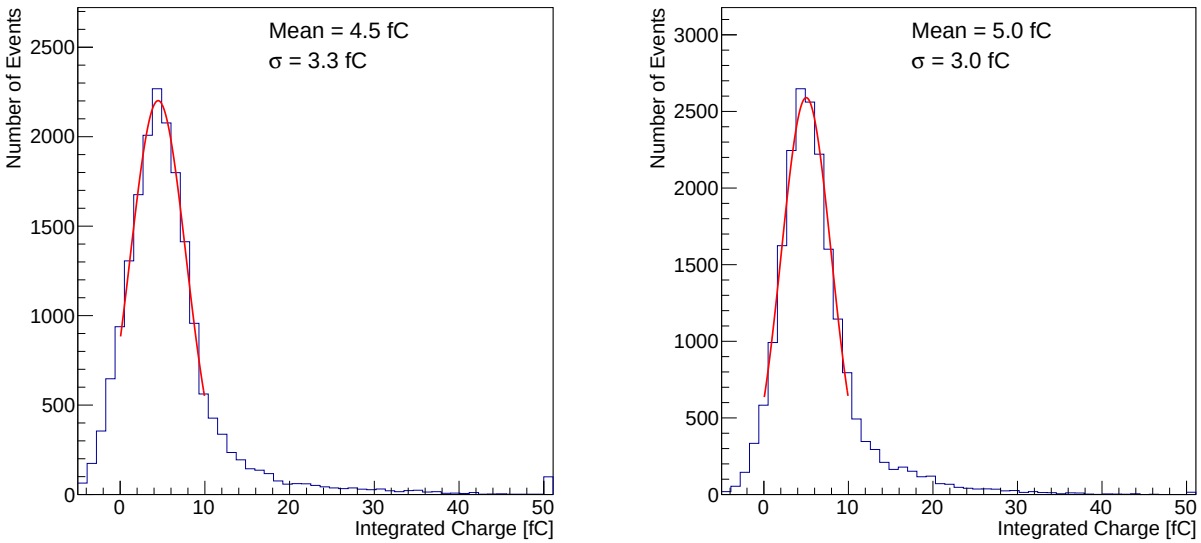

Figure 7: The distribution of charge integrated in the silicon sensor is shown for a beam of 120 GeV protons (left) and 8 GeV electrons (right) without any absorber upstream of the silicon sensor. These conditions mimic the response of the silicon sensor to a minimum-ionizing particle.

integrated charge distribution measured in the silicon sensor after 6 radiation lengths of tungsten for 32 GeV electrons. We plot the mean and RMS of these distributions as a function of incident electron beam energy in Figure 9. The uncertainties plotted show the RMS of the charge distribution. We observe a fairly linear depedence between the measured charge and the incident beam energy, for beam energies between 4 GeV and 32 GeV.

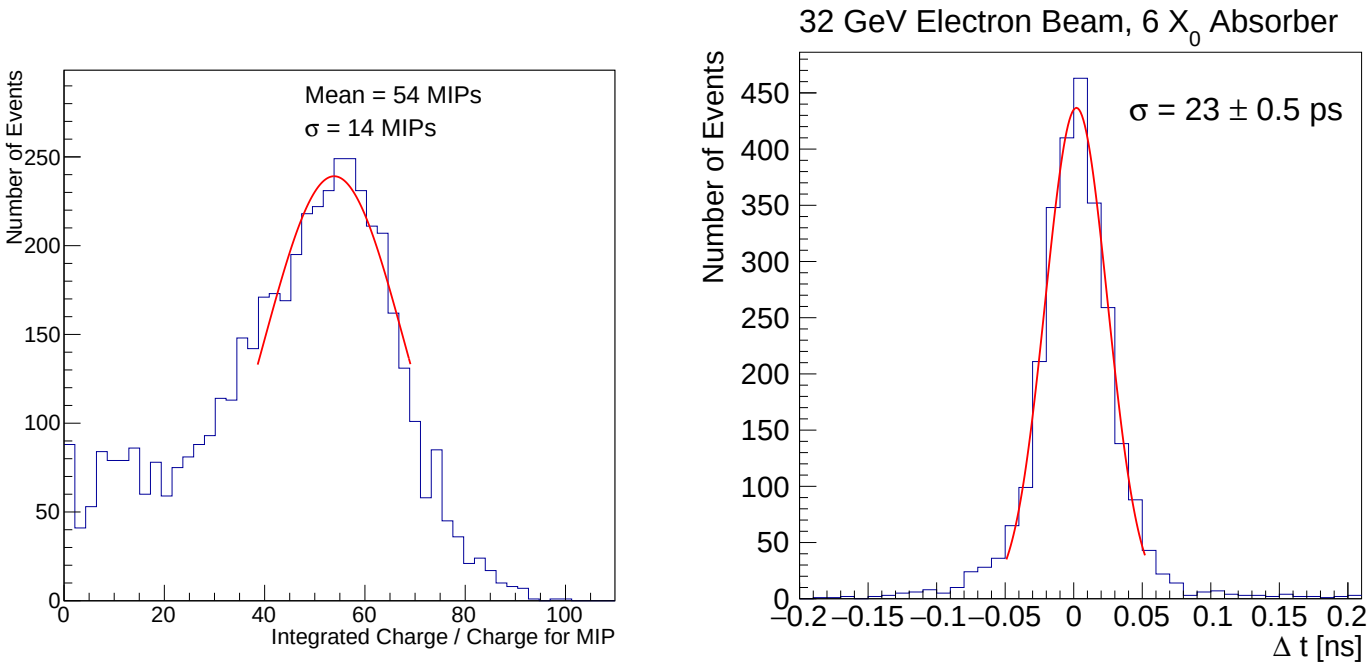

Figure 8: An example of the distribution of integrated charge in the silicon sensor is shown in units of the charge measured for MIP's. A 32 GeV electron beam is used, and the silicon sensor is placed after 6 radiation lengths of tungsten absorber.

We also measure the time resolution between the silicon sensor and the Photek MCP-PMT. An example of the time of flight distribution is shown on the right of Figure 8 for 32 GeV electrons after 6 radiation lengths of tungsten. The dependence of the measured time resolution on the beam energy is shown on the right of Figure 9. We observe an improvement in the time resolution as beam energy increases, and achieve a time resolution of 23 ps for the 32 GeV electron beam.

Furthermore, we study the response and time resolution of the silicon sensor along the longitudinal direction of the shower development. We measure the integrated charge and the time resolution as a function of the absorber thickness and present the results in Figure 10. A typical longitudinal shower profile is observed, consistent with previous studies performed using a secondary emission calorimter prototype based on MCP's [**?**], as well as independent studies of silicon-based calorimeter prototypes [**?**]. We also observe that the time resolution improves as the shower develops towards its maximum in the longitudinal direction.

Finally, we studied the dependence of the time resolution as a function of the bias voltage applied to deplete the silicon sensor. The measurements are shown in Figure 11 for 16 GeV electrons after 6 radiation lengths of tungsten absorber. We find that the time resolution improves as the bias voltage is increased, which is expected on the basis of increased velocity of electrons and holes in silicon at larger bias voltage.

5 Discussion

From Figures 6 and 7, we observe that the noise of the prototype system is sufficiently low to extract signals from MIPs. Comparing the RMS of the noise distribution with the mean of the MIP signal,

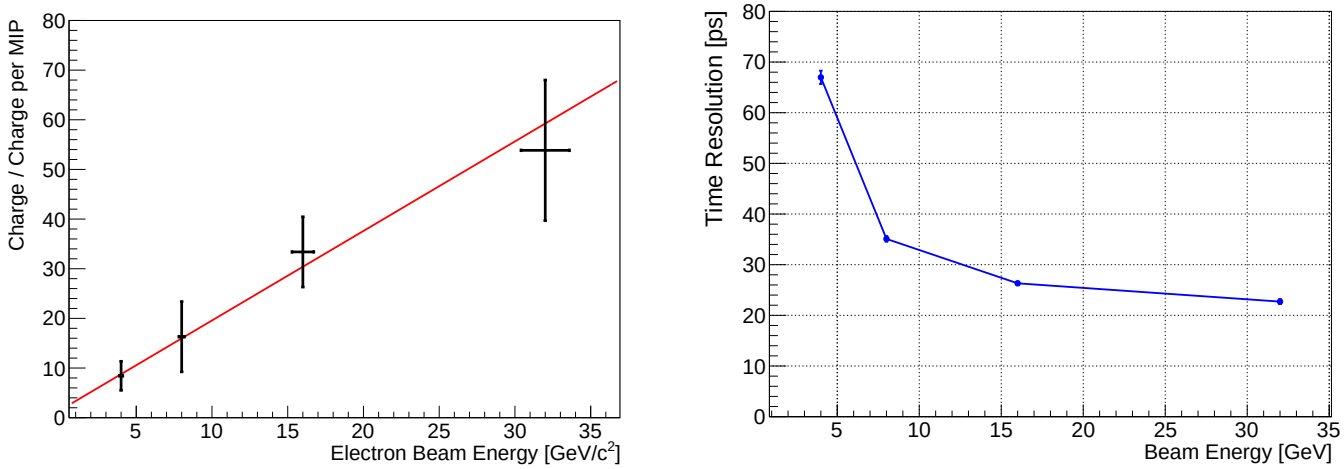

Figure 9: On the left, the integrated charge in the silicon sensor expressed in units of the charge measured for MIP's is shown as a function of the electron beam energy. The uncertainty bands show the RMS of the measured charge distribution. The red line is the best fit to a linear function. On the right, the measured time resolution between the silicon sensor and the Photek MCP-PMT reference is shown as a function of the electron beam energy.

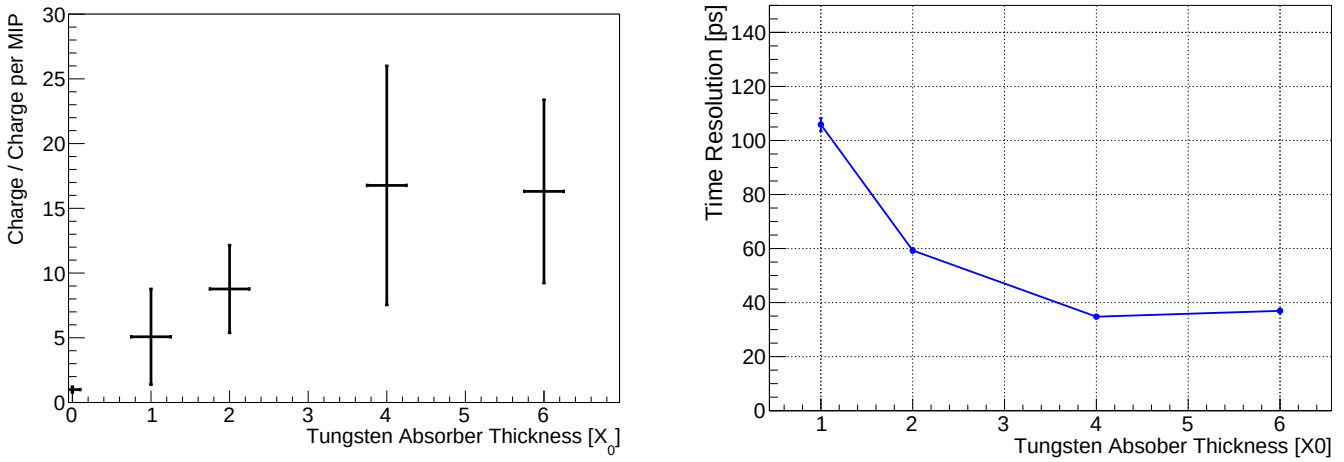

Figure 10: On the left, the integrated charge in the silicon sensor expressed in units of the charge measured for MIP's is shown as a function of the absorber (W) thickness measured in units of radiation lengths (X_0). The uncertainty bands show the RMS of the measured charge distribution. On the right, the time resolution between the silicon sensor and the Photek MCP-PMT reference is shown as a function of the absorber thickness.

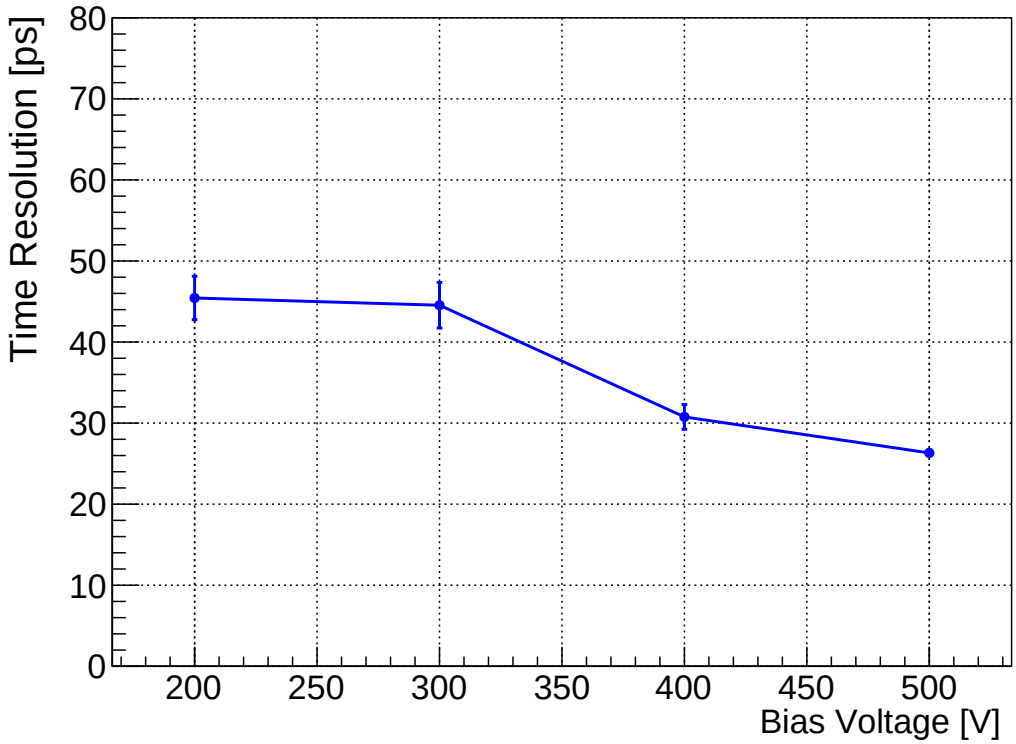

Figure 11: The time resolution between the silicon sensor and the Photek MCP-PMT reference is shown as a function of bias voltage applied on the silicon sensor.

we find a signal-to-noise ratio around 2 to 2.5. A rough estimate from Figure 7 demonstrates that the efficiency to detect 120 GeV protons and 8 GeV electrons with no absorber present is larger than 80%. Based on the measurements for MIPs, we derive signal distributions for electromagnetic showers normalized to MIP response, and observe a relatively linear response to the electron beam energy after 6 radiation lengths of tungsten absorber in Figure 9. We also measure a longitudinal shower profile in Figure 10 that is consistent with similar past measurements. Having established standard calorimetric properties of the prototype, we proceed to study the timing properties.

We begin with some general considerations of timing in silicon. An electric field applied to silicon results in a built-in junction voltage (0.6V) which is typical of silicon diodes. The high electric field in silicon leads to total depletion as all free charge carriers are removed. When charged particles pass through the totally depleted region in silicon, it ionizes atoms and produces electron-hole pairs which serve as charge carriers. The electrons are collected on positive electrode and the holes are collected on the negative electrode. The time and jitter associated with relativistic particles traversing through the silicon material can be neglected as it takes less than 1 ps for relativistic particles to pass through the full 300 μm of silicon material. At high electric field (more than 105 V/cm), the mobility of carriers attain a constant drift velocity of 108 mm/s (or about 1μm/10 ps) in the silicon material [**?**]. The amount of electrons produced in the 100 um is 10000. The time needed to collect all electrons in the 100 um is 1ns. The electrons produced closer to the positive electrode collected first. The time needed to pass 1 μm by electron is $\sim$10 ps. The average time between the electrons is $\sim$1 ps. If electronic can detect 100 electrons its arrival time could be inside of the 10 ps. The time jitter could be estimated as 3 ps for Poisson timing distribution. For example, if electronics can detects $\sim$100 electrons (with additional amplification) produced in silicon they collected from the thickness of $\sim$10 μm. We can say that the "rest of the silicon thickness" does not participate in the silicon time jitter, because these electrons are coming "too late". This simple model can explain in general obtained test beam results.

Our results show that the time stamp associated with electromagnetic showers induced by electrons with energy between 20 GeV and 30 GeV can be measured with a precision better than 25 ps. Subtracting for the resolution of the reference Photek MCP-PMT detector yields a precision better than 20 ps. Moreover, we observe an improvement of the time resolution with the energy of the electron, and more generally with an increase in the signal amplitude. These measurements demonstrate that a calorimeter based on silicon sensors as the active medium can achieve intrinsic time resolution at the 20 ps level, as long as noise is kept under control. Time jitter arising from intrinsic properties of the silicon sensor is demonstrated to be well below the 20 ps level.

6 Conclusion

We obtained a best time resolution measurement for silicon sensors of 23 ps, using a beam of 32 GeV electrons and with the silicon sensor placed after 6 radiation lengths of tungsten absorber. Based on our calibration data for the response of the silicon sensor to MIPs, this measurement corresponds roughly to 54 secondary particles registered from the electromagnetic shower. We observe a roughly linearly increasing response as the energy of the electron beam is increased, and we observe a longitudinal shower profile consistent with similar past measurements. This result yields further encouragement to use silicon as active layer in calorimeters, as is planned for example for the CMS Phase 2 upgrade [**?**], and explicitly demonstrates the opportunity to use silicon for timing measurements in future calorimeters. In the future, we plan to extend our studies to more realistic prototypes covering larger transverse and longitudinal regions of the electromagnetic shower and using multiple channels.

7 Acknowledgements

We thank the FTBF personnel for very good beam condition during our test beam run. We also appreciate the technical support of the Fermilab SiDet department for the production of high quality silicon samples. We appreciate Helmuth Spieler monography as a good source of silicon information [**?**].